Heterogeneous magnetism in Fe-doped bulk-amorphous and nanostructured Pd-based alloys

2008 J. Phys.: Condens. Matter 20 015211

(http://iopscience.iop.org/0953-8984/20/1/015211)

J. Phys.: Condens. Matter **20** (2008) 015211 (8pp) doi:10.1088/0953-8984/20/01/015211

Heterogeneous magnetism in Fe-doped bulk-amorphous and nanostructured Pd-based alloys

L F Kiss[1], T Kemény[1], L Bujdosó[1], I Bakonyi[1], S Baskoutas[2], P Poulopoulos[2], V Kapaklis[3] and C Politis[3,4]

[1] Research Institute for Solid State Physics and Optics, Hungarian Academy of Sciences, H-1525 Budapest, PO Box 49, Hungary
[2] Department of Materials Science, University of Patras, Patras 26504, Greece
[3] Engineering Sciences Department, School of Engineering, University of Patras, Patras 26500, Greece
[4] Forschungszentrum Karlsruhe, Institut für Nanotechnologie, PO Box 3640, Karlsruhe 76021, Germany

E-mail: kissl@szfki.hu

Received 13 September 2007
Published 5 December 2007
Online at stacks.iop.org/JPhysCM/20/015211

Abstract

It has been shown in a previous work (Kapaklis *et al* 2005 *J. Appl. Phys.* **98** 044319) that whereas the alloy composition $Pd_{40}Cu_{30}Ni_{10}P_{20}$ can be easily cast as a bulk metallic glass, a partial replacement of Pd by Fe ($Pd_{35}Cu_{30}Ni_{10}Fe_5P_{20}$) leads to a significant crystalline fraction under the same casting conditions. In order to understand the formation and properties of these precipitates, fully amorphous ribbons of both alloy compositions were also prepared by conventional melt-spinning. Magnetic data reveal that doping with 5 at.% iron leads to the formation of nanosized crystalline inclusions in the residual bulk amorphous matrix which are completely absent in the ribbon melt-spun from the same ingot. In both types of Fe-containing alloys the amorphous matrix contains giant moments. Their size is of a few hundred (ingot) and a few tens (ribbon) of Bohr magnetons. The iron-free alloy corrected for the Langevin diamagnetism shows Pauli paramagnetism with similar susceptibility values in both the ingot and the ribbon. These values are close to the Pauli susceptibility of a control sample, a melt-spun $Pd_{82}P_{18}$ alloy which is expected to be as homogeneous as the typical binary amorphous alloys. The possible origin of different, controversial magnetic behaviors reported in the literature for Fe-doped Pd-based bulk and melt-spun alloys is discussed.

1. Introduction

Recently, there has been a growing interest in producing bulk metallic glasses (BMG) because their shapes can be tailored easily for various applications in contrast to other production methods (melt-spinning, vacuum evaporation, molecular beam epitaxy, etc) which offer amorphous alloys with limited geometries (ribbons of around 10 μm thickness, thin layers several nanometers thick). Moreover, the advantageous magnetic properties of the bulk metallic glasses can be combined with their good mechanical properties which can be further strengthened by precipitating nanocrystalline inclusions in the bulk amorphous matrix. While research has been mainly focused on identifying those factors controlling glass formation, the possible influence of a small but non-negligible quantity of crystalline precipitates usually unavoidably present due to the limited cooling rates applied for bulk glass formation is far from being understood. Therefore, further studies are needed to reveal how the crystalline fraction present in the amorphous matrix affects the structure and various properties including also magnetic behavior.

The experimental detection of a small quantity of (nano)crystalline precipitates in BMGs is by no means an easy task. The magnetic properties, however, are extremely sensitive to the presence of such precipitates, and therefore a magnetic study provides a relatively simple and cheap method

to reveal some aspects of structural heterogeneity. Besides this practical advantage, the study of the magnetic properties in BMGs is also of theoretical importance. The very complex magnetic behavior of some BMGs (e.g. Fe-containing Pd-based alloys) is often interpreted as an intrinsic feature of a structurally homogeneous amorphous alloy. In this paper we will show that the presence of known nanocrystalline precipitates in BMGs can lead to similar complex magnetic behavior without assuming any exotic magnetic interactions (peculiar magnetic phase diagrams) in the material.

Pd–Ni–P-based amorphous alloys have good glass-forming ability and have been produced since the 1980s. Drehmann and Greer described the kinetics of crystal nucleation and growth in a $Pd_{40}Ni_{40}P_{20}$ glass [1]. Bulk glassy $Pd_{40}Ni_{10}Cu_{30}P_{20}$ alloys were prepared in the form of ingots [2, 3] and their thermal behavior was also investigated [4]. Bulk glass formation was studied in the Pd–Ni–P system produced by a flux-melting and water-quenching method in a wide concentration range [5–7]. Among these alloys the magnetic [8], magnetocaloric [9] and structural [10] properties of 7 mm diameter glassy rods of $Pd_{40}Ni_{40-x}Fe_xP_{20}$ ($0 \leqslant x \leqslant 20$) were investigated in greater detail. These latter bulk alloys were shown to be x-ray amorphous in all cases, except for $x \geqslant 20$ where crystalline inclusions were found [8, 10]. The magnetic properties of these bulk alloy series are very similar to those of our $Pd_{35}Cu_{30}Ni_{10}Fe_5P_{20}$ and $Pd_{40}Cu_{30}Ni_{10}P_{20}$ ingots. Shen *et al* found [8] that Fe-free amorphous $Pd_{40}Ni_{40}P_{20}$ ($x = 0$) is paramagnetic at all temperatures. The low-field magnetization of bulk $Pd_{40}Ni_{40-x}Fe_xP_{20}$ ($5 \leqslant x \leqslant 17.5$) alloys showed a cusp as a function of temperature, which was attributed to a transformation from paramagnetic to superparamagnetic to spin-glass states with decreasing temperature. Moreover, these authors also stated that bulk amorphous $Pd_{40}Ni_{22.5}Fe_{17.5}P_{20}$ exhibits a field-induced ferromagnetic-like state that separates the superparamagnetic state at higher temperatures and the spin-glass state at lower temperatures. Later, the $Pd_{40}Ni_{40-x}Fe_xP_{20}$ ($5 \leqslant x \leqslant 20$) series including the above discussed composition was also prepared as melt-spun ribbons and their magnetic properties were investigated mainly by Mössbauer spectroscopy [11, 12]. The bulk magnetic properties were mentioned only briefly without showing any figures and were claimed to be similar to those of the bulk amorphous ingot. Very recently [13] neutron depolarization studies on the same ribbon revealed a correlation length of 200 Å (20 nm) between the magnetic moments.

In a recent publication [14], Hsiao *et al* have pointed out that the same alloy ($Pd_{40}Ni_{22.5}Fe_{17.5}P_{20}$) produced by melt-spinning using a high quenching rate shows evidence of chemical segregation on the nanoscale in the as-solidified state. They claim that for the melt-spun alloy the non-saturating $M(H)$ curves and the complex set of magnetic transitions similar to those observed in the bulk ingot [8] must have their root in its nanoscale structure. The diameter of the spherical superparamagnetic cluster of a hypothesized $(Pd, Fe, Ni)_3P$ structural unit containing $\mu = 7700\ \mu_B$ at $T = 50$ K was estimated to be $D = 3.4$ nm which is too small to be detected by x-ray diffraction methods and may be difficult to detect by electron microscopy [14].

We have recently reported [15] on the formation and the structural, thermal and elastic properties of Pd-based bulk amorphous ($Pd_{40}Cu_{30}Ni_{10}P_{20}$) and nanostructured ($Pd_{35}Cu_{30}Ni_{10}Fe_5P_{20}$) alloys. Element-specific near-edge x-ray absorption fine-structure spectroscopy (NEXAFS) provided information on the electronic structure and local symmetry properties of these samples [16]. These investigations [15, 16] found small nanocrystalline inclusions in the bulk alloy containing 5 at.% Fe and revealed that the most probable crystalline phases are a $(Fe_{1-x}Ni_x)_2P$ hexagonal structure and a Cu-rich face-centered-cubic solid solution. Whereas the actual composition of the $(Fe_{1-x}Ni_x)_2P$ precipitates could not be clarified, it was established that about 40% of Cu is in the Cu-rich phase that may contain about 2 at.% Pd as well.

In this paper, we report on the magnetic properties of bulk $Pd_{40}Cu_{30}Ni_{10}P_{20}$ and $Pd_{35}Cu_{30}Ni_{10}Fe_5P_{20}$ alloys. In order to clarify the complex magnetic nature found in these alloys, the ingots were also melt-spun on a rotating copper wheel. The resulting ribbons, with a thickness of around 10 μm, are expected to have a fairly homogeneous amorphous structure. The magnetic properties of an amorphous $Pd_{82}P_{18}$ ribbon prepared by melt-spinning were also investigated. This metallic glass does not contain either Fe or Ni atoms which are inclined to polarize surrounding Pd atoms and, therefore, it is considered as a completely homogeneous, amorphous control sample.

2. Experimental details

The preparation of bulk $Pd_{40}Cu_{30}Ni_{10}P_{20}$ and $Pd_{35}Cu_{30}Ni_{10}Fe_5P_{20}$ alloys in the form of ingots was described in detail elsewhere [15]. The ribbons were prepared from the same ingots by melt-spinning under vacuum. A $Pd_{82}P_{18}$ alloy was also melt-spun into a ribbon 1.9 mm wide and 22 μm thick. All the samples were shown to be amorphous by x-ray diffraction, differential scanning calorimetry (DSC) and/or Mössbauer spectroscopy, except the Pd-based ingot doped with 5 at.% Fe which contained nanosized crystalline inclusions in the amorphous matrix.

The calorimetric measurements were performed in a Perkin-Elmer DSC-2 based differential scanning calorimeter with home-made electronics in the temperature range of 350–1000 K. The magnetic properties were measured with the help of a Quantum Design MPMS 5S superconducting quantum interference device (SQUID) magnetometer in a temperature and field range of $5\ \text{K} \leqslant T \leqslant 300\ \text{K}$ and $0 \leqslant H \leqslant 5$ T, respectively. For the magnetic measurements, an ingot sample with a mass of around 20 mg was placed in a gelatin capsule, while for the ribbon samples several pieces with a total mass of less than 1 mg were mounted on the surface of a silicon wafer using vacuum grease. The mass of the $Pd_{82}P_{18}$ ribbon used as a control sample was 16.61 mg. For the iron-free alloys, the signal of the sample holder constituted a considerable fraction of the total signal (~90%), therefore the sample holders were measured separately with the highest available precision for correction. The ZFC (zero-field cooled) magnetization was measured on warming the sample at a given applied field

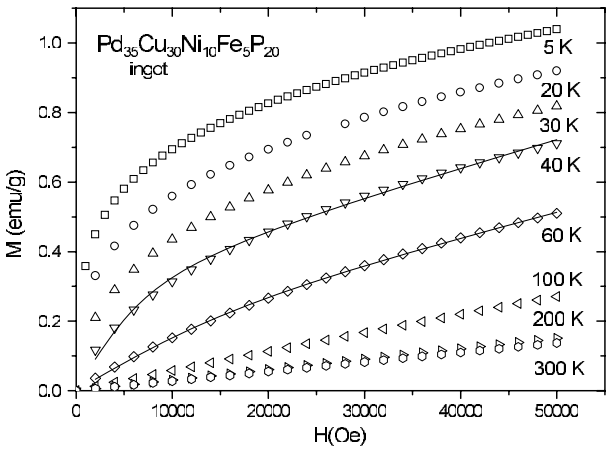

Figure 1. Magnetization as a function of applied field measured at various temperatures for the bulk $Pd_{35}Cu_{30}Ni_{10}Fe_5P_{20}$ ingot. The solid lines are fits to equation (1).

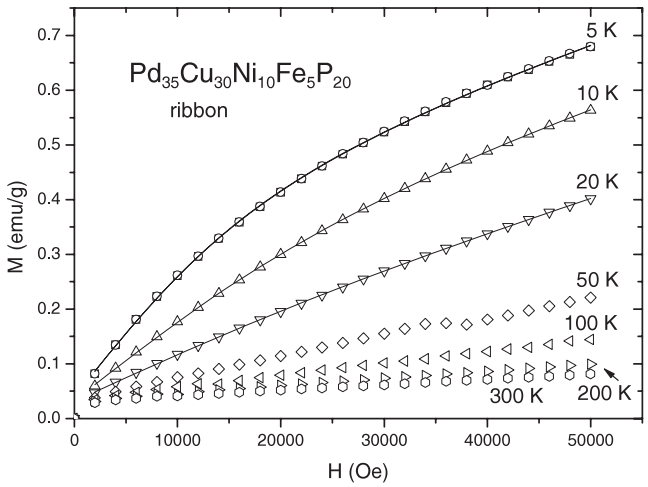

Figure 2. Magnetization as a function of applied field measured at various temperatures for the melt-spun $Pd_{35}Cu_{30}Ni_{10}Fe_5P_{20}$ ribbon. The solid lines are fits to equation (1).

after the sample had been cooled from $T = 300$ to 5 K in the remanence field of the superconducting magnet (less than $H_{\rm rem} = -1$ Oe). The field-cooled (FC) magnetization was measured in the same way, except that the cooling was performed in a magnetic field equal to the measuring field.

3. Results

The calorimetric results are summarized in table 1. The addition of 5 at.% iron does not alter significantly the glass-transition temperature. The calorimetric data of the iron-free Pd-based alloy agreed well with the literature [2, 3, 17, 4]. The small enthalpy value for the crystallization of the bulk $Pd_{35}Cu_{30}Ni_{10}Fe_5P_{20}$ ingot with respect to the ribbon of the same composition reflects our previous findings [15, 16] in that the ingot contains nanosized crystalline inclusions embedded in the amorphous matrix.

Figure 1 shows the magnetization of the $Pd_{35}Cu_{30}Ni_{10}Fe_5P_{20}$ ingot as a function of the applied magnetic field. No saturation is observed even at our highest applied field of $H = 50$ kOe. This behavior is very similar to that found in the literature for similar compositions (but without Cu) [8, 14]. The magnetization can be adequately described as a function of the applied field (H) and temperature (T) by the sum of a Langevin function, a term of high-field susceptibility and a constant:

$$M(H,T) = N_\mu \mu \left(\coth \frac{\mu H}{k_{\rm B} T} - \frac{k_{\rm B} T}{\mu H} \right) + \chi_{\rm hf} H + M_0, \quad (1)$$

where μ is the average magnetic moment of magnetic clusters to be specified later, N_μ is the density of the clusters, $\chi_{\rm hf}$ is a high-field susceptibility component and $k_{\rm B}$ is Boltzmann's constant. M_0 is a constant (less than 5% of the saturation magnetization in the Fe-containing alloys) and is attributed to a small amount of ferromagnetic Ni(Fe)-rich precipitates. The fitted magnetic moment, μ, shows a sharp temperature dependence: it has a maximum around $T = 23$ K, varying from $\mu = 274$ to 192 $\mu_{\rm B}$ between $T = 20$ and 40 K. At $T = 5$ K μ is much smaller ($\mu = 78$ $\mu_{\rm B}$), indicating that some of the magnetic clusters are blocked. Above $T = 40$ K the total magnetization of the clusters, N_μ μ, decreases rapidly and becomes zero at around $T = 100$ K, suggesting that this temperature is close to the Curie point of the clusters. The fitted curves for two temperatures are shown in figure 1 and from the fits with one of the highest μ, the values of the fitted parameters, N_μ, μ, $\chi_{\rm hf}$ and M_0, are given at $T = 40$ K in table 1. The value of $\mu = 192$ $\mu_{\rm B}$ obtained for the $Pd_{35}Cu_{30}Ni_{10}Fe_5P_{20}$ ingot hints at the presence of magnetic clusters which determine the high-field behavior of the alloy.

The $M(H,T)$ curves for the $Pd_{35}Cu_{30}Ni_{10}Fe_5P_{20}$ ribbon are plotted in figure 2. At low temperatures, they saturate in an even lesser degree than for the ingot of the same composition (see figure 1). The fits to equation (1) are shown for three temperatures in figure 2. The temperature dependence of the fitted magnetic moment, μ, shows a much sharper maximum at $T = 20$ K compared to that of the ingot. The Curie point of the magnetic clusters (where the total magnetization of the clusters disappears) is also much lower ($T \sim 50$ K). The parameters of the fit (N_μ, μ, $\chi_{\rm hf}$ and M_0) to equation (1) at $T = 20$ K are given in table 1. Note that the average magnetic moment of $\mu = 23$ $\mu_{\rm B}$ obtained from the fit is almost one order of magnitude smaller than that for the ingot.

In figure 3 the (identical) ZFC and FC magnetizations for the $Pd_{35}Cu_{30}Ni_{10}Fe_5P_{20}$ ribbon are shown as a function of temperature measured at a constant applied field of $H = 5$ kOe, together with the magnetization versus temperature (shown as an inset in figure 3) taken at $H = 6$ kOe from the $M(H,T)$ curves of the ingot of the same composition displayed in figure 1. For both samples, the $M(T)$ curve could be described (see solid lines in figure 3) in the whole temperature range by the sum of a Curie–Weiss term and a small constant. The Curie–Weiss temperature is close to zero (of the order of a few K). From the fits, the molar Curie

Table 1. Thermal and magnetic characteristics of the alloys investigated: M', molar mass; T_g, glass-transition temperature; T_x, onset of crystallization; ΔH, crystallization enthalpy; μ, magnetic-cluster moment from equation (1); N_μ, mass density of magnetic clusters from equation (1); χ_{hf}, high-field susceptibility from equation (1); M_0, magnetic moment of impurities from equation (1); μ_{eff}/Fe, effective magnetic moment per Fe atom from equation (2); μ_{eff}/cluster, effective magnetic moment per magnetic cluster; χ_{dia}, diamagnetic susceptibility of the ion cores; χ^0_{exp}, susceptibility calculated by fitting to the high-field portion of the $M(H)$ curve and extrapolated to $T = 0$; $\chi^0_{cond} = \chi^0_{exp} - \chi_{dia}$, conduction electron susceptibility.

Material	$Pd_{35}Cu_{30}Ni_{10}Fe_5P_{20}$		$Pd_{40}Cu_{30}Ni_{10}P_{20}$		$Pd_{82}P_{18}$
M', molar mass (g)	71.161 91		73.689 56		92.823 284
Form	Ingot	Ribbon	Ingot	Ribbon	Ribbon
T_g (K)	577	593	578	586	—
T_x (K)	640	620	657	660	582
ΔH (J g^{-1})	23.5	67	50.5	50.8	49
μ (μ_B)	192[a]	23[b]	5.8[c]	—	—
N_μ (10^{17} g^{-1})	2.01[a]	4.9[b]	1.0[c]	—	—
χ_{hf} (10^{-6} emu/gOe)	7.7[a]	4.0[b]	−0.14[c]	—	—
M_0 (10^{-2} emu g^{-1})	0[a]	3.1[b]	0.062[c]	—	—
μ_{eff}/Fe (μ_B)	4.50	1.41	—	—	—
μ_{eff}/cluster (μ_B)	207	43	—	—	—
χ_{dia} (10^{-6} emu/molOe)	—	—	−20.95	−20.95	−26.83
χ^0_{exp} (10^{-6} emu/molOe)	—	—	−11.8	2.61	$\geqslant -4.79$
χ^0_{cond} (10^{-6} emu/molOe)	—	—	9	23.6	22

[a] At $T = 40$ K.
[b] At $T = 20$ K.
[c] At $T = 5$ K.

constant

$$C_M = \frac{N\mu_{eff}^2}{3k_B} \tag{2}$$

can be deduced where μ_{eff} is the effective moment and N is Avogadro's number. The μ_{eff} values per iron atom calculated from C_M are given in table 1. The figure of $\mu_{eff} = 4.50\ \mu_B$ per Fe atom found in the ingot is almost equal to that deduced for the $Pd_{40}Ni_{22.5}Fe_{17.5}P_{20}$ bulk metallic glass in [8]. It suggests a strong spin polarization of neighboring Pd atoms around Fe atoms. In crystalline Pd(Fe) solid solutions, the Fe atoms cause an even stronger spin polarization of the Pd matrix atoms with μ_{eff} per Fe atom of the order of 12 μ_B [18]. In the $Pd_{35}Cu_{30}Ni_{10}Fe_5P_{20}$ ribbon, a smaller value of $\mu_{eff} = 1.41\ \mu_B$ per Fe atom is deduced, which is in line with the smaller degree of inhomogeneity in the ribbon.

The calculation of the effective moment per Fe atom is, however, misleading because it suggests that individual Fe atoms and their polarized Pd neighbors carry independent magnetic moments. In fact, the concentration of the magnetic clusters responsible for the slowly saturating $M(H)$ curves (figures 1 and 2) is much smaller. It is calculated to be $x_{cl} = 23.7$ and 57.7 ppm for the ingot and the ribbon, respectively, as deduced from the fitted parameter N_μ (table 1) by $x_{cl} = N_\mu\ M'/N$ where M' is the molar mass. Assuming that these clusters carry the magnetic moments instead of individual Fe atoms, $\mu_{eff} = 207$ and 43 μ_B per cluster is obtained for the ingot and the ribbon, respectively. These values (also given in table 1) are very close to those calculated from the Langevin fit of the respective $M(H)$ curves ($\mu = 192$ and 23 μ_B for the ingot at $T = 40$ K and for the ribbon at $T = 20$ K, respectively). This consistency strongly suggests that the high-field behavior of both the ingot and the ribbon of the Fe-containing Pd-based alloy is determined by these magnetic clusters.

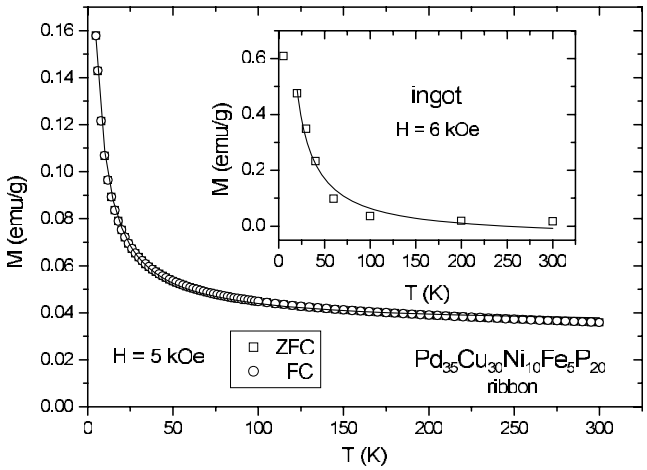

Figure 3. ZFC and FC magnetization as a function of temperature measured at $H = 5$ kOe for the melt-spun $Pd_{35}Cu_{30}Ni_{10}Fe_5P_{20}$ ribbon. Inset: magnetization versus temperature measured at $H = 6$ kOe for the bulk $Pd_{35}Cu_{30}Ni_{10}Fe_5P_{20}$ ingot. The solid lines are fits to the Curie–Weiss law (plus a constant).

It is evident from the above observations that the overall (high-field) magnetic behavior of the fully amorphous ribbon and the partly crystalline ingot is very similar. Consequently, if a BMG ingot contains some crystalline fraction it should not have a significant influence on the high-field magnetic characteristics. As we shall see, the crucial point will be the low-field magnetic behavior at low temperatures.

Figure 4 shows the ZFC and FC magnetization of both the $Pd_{35}Cu_{30}Ni_{10}Fe_5P_{20}$ ingot and ribbon as a function of temperature measured at low applied fields ($H = 10$ Oe). For the ingot, a cusp-like ZFC curve can be observed with

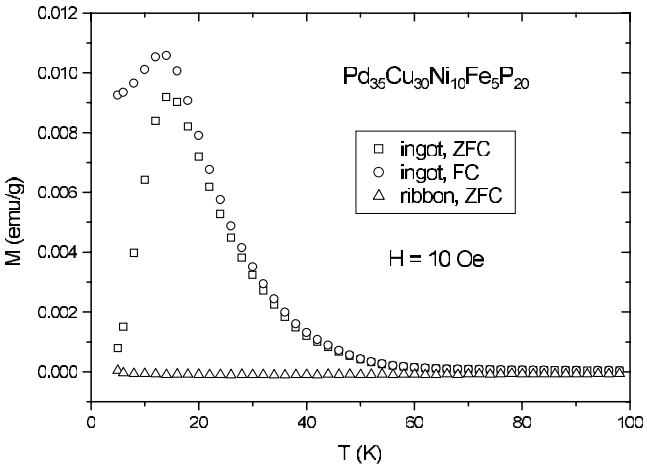

Figure 4. ZFC and FC magnetization as a function of temperature measured at $H = 10$ Oe for the bulk $Pd_{35}Cu_{30}Ni_{10}Fe_5P_{20}$ ingot and the melt-spun ribbon of the same composition.

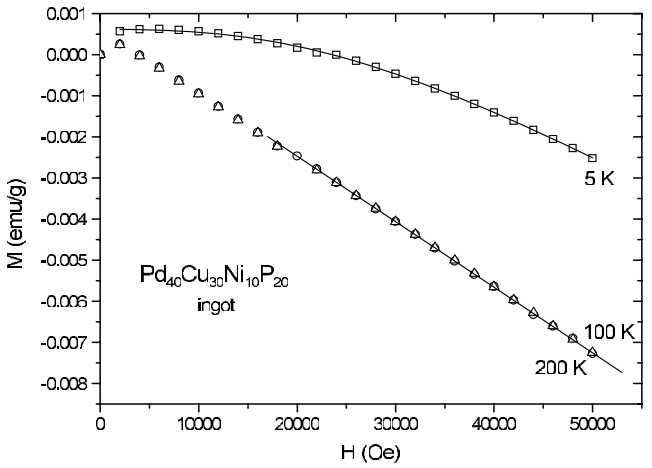

Figure 5. Magnetization as a function of applied field measured at various temperatures for the bulk $Pd_{40}Cu_{30}Ni_{10}P_{20}$ ingot. The solid line at $T = 5$ K is a fit to equation (1) while that at $T = 200$ K is a linear fit between $H = 20$ and 50 kOe.

a maximum at 14 K. Above this temperature the FC and ZFC curves coincide, below 14 K the FC curve deviates from the ZFC one and saturates after a small maximum with decreasing temperature. Similar behavior was reported for bulk amorphous Pd–Ni–Fe–P alloys [8] and also for a $Pd_{40}Ni_{22.5}Fe_{17.5}P_{20}$ melt-spun alloy [14]. In contrast, the ribbon produced from the ingot of the same composition shows no effect in the same temperature range (zero magnetization, see triangle symbols in figure 4). The cusp-like feature found at small fields is, therefore, not an intrinsic feature of the studied Fe-containing Pd-based ingot but it is a consequence of its excessive heterogeneity (large crystalline fraction). It is known that the ingot contains a large quantity of nanocrystalline precipitates inside the amorphous matrix [15, 16]. As the amorphous melt-spun ribbon does not show a cusp-like behavior, this feature of the bulk alloy is a manifestation of the thermal blocking of the superparamagnetic precipitates present in the amorphous matrix of the ingot. Using the observed blocking temperature of $T_B = 14$ K, the diameter of the assumed spherical precipitates can be estimated from the balance of the thermal and anisotropy energy ($KV \sim 25k_BT_B$, where V is the average volume of the precipitates). Since the precipitates consist in fact of the $(Fe_{1-x}Ni_x)_2P$ phase [15, 16], an estimate for D could be obtained knowing the anisotropy constant for this phase. The magnetic properties of $(Fe_{1-x}Ni_x)_2P$ compounds are well documented in the literature. It was shown [19] that Fe_2P ($x = 0$) is a ferromagnet with a Curie temperature $T_C = 209$ K and there is a T_C maximum ($T_C = 342$ K) versus x at $x = 0.08$ while the dominant magnetocrystalline anisotropy constant, K_1, decreases rapidly with increasing x from an unusually large value, $K_1 = 2.32 \times 10^7$ erg cm^{-3} at $x = 0$ and $T = 4.2$ K, and becomes almost zero near $x = 0.3$. TEM observations [15] indicated the actual size of the precipitates between $D = 10$ and 50 nm. From these values, anisotropy constants of $K \sim 9.2 \times 10^4$ and 740 erg cm^{-3}, respectively, can be deduced. Taking into account the composition dependence of K_1 and T_C for the $(Fe_{1-x}Ni_x)_2P$ compound [19], the Ni content of the $(Fe_{1-x}Ni_x)_2P$ precipitates can be roughly estimated to be between $0.4 < x < 0.6$. Independently of these precipitates, the amorphous matrix of both the ingot and the ribbon of the Fe-doped Pd-based alloy contains magnetic moments which are responsible for the non-saturating feature of the high-field magnetization curves (figures 1 and 2). These magnetic units are the giant moments well known from dilute PdFe alloys (see [18] and references therein).

A completely different magnetic behavior is found for the Fe-free Pd-based alloy ($Pd_{40}Cu_{30}Ni_{10}P_{20}$). Figure 5 shows the magnetization as a function of the applied field for the bulk amorphous ingot. Except at $T = 5$ K, a nearly temperature-independent signal is only observed giving a susceptibility of $\chi^0_{exp} = -11.8 \times 10^{-6}$ emu/molOe (table 1). Here χ^0_{exp} is the susceptibility calculated by fitting the high-field portion of the $M(H)$ curve and extrapolated to $T = 0$.

For non-magnetic metals, when neglecting spin–orbit coupling, the total magnetic susceptibility, χ_{tot}, consists of a spin and an orbital term. Both terms are usually temperature independent, although the spin susceptibility originating from the Pauli paramagnetism (χ_P) of conduction electrons may exhibit a weak quadratic temperature dependence. The orbital susceptibility, χ_{orb}, was shown [20] to contain three contributions. The first one is the Langevin diamagnetic susceptibility, χ_{dia}, calculated [21] for metals up to the atomic number 46 and we have used these values here for Pd, Cu, Ni and Fe, whereas for P we have taken the ionic value as given by Selwood [22] for the P^{5+} ion. The second orbital term, the Van Vleck paramagnetic susceptibility, and the third term, the Landau-type orbital susceptibility of the conduction electrons, can be safely neglected here. It is perhaps a more appropriate approach here just to define a conduction electron susceptibility, χ_{cond} by writing $\chi_{exp} = \chi_{tot} = \chi_{dia} + \chi_{cond}$. Thus the susceptibility, χ_{cond}, may be considered as corresponding mainly to the Pauli susceptibility, χ_P, at least apart from some small unknown orbital corrections which, nevertheless, can be considered practically the same for all the alloys we investigate

here and therefore allow for a proper comparison of the various alloys.

When corrected for the diamagnetic susceptibility as described above, we obtain a conduction electron susceptibility of $\chi^0_{\rm cond} = 9 \times 10^{-6}$ emu/molOe (extrapolated to $T = 0$, table 1) for the amorphous $Pd_{40}Cu_{30}Ni_{10}P_{20}$ ingot.

The magnetization curve measured at $T = 5$ K can be described by equation (1) (solid line) giving a magnetic moment of $\mu = 5.8\ \mu_B$. This small cluster moment can be related to small conglomerates of Ni atoms which are inclined to form giant moments [23]. The saturation magnetization of these conglomerates ($M_{\rm sat} \sim 0.005$ emu g^{-1}) is less than the magnetization change due to the diamagnetic component of the amorphous matrix, which explains the negative magnetization values measured at high fields. The Curie point of these conglomerates should be much less than $T = 100$ K since no sign of a Langevin-function component in the $M(H)$ curve can be seen at and above this temperature.

The Langevin-function component is absent even at $T = 5$ K for the $Pd_{40}Cu_{30}Ni_{10}P_{20}$ ribbon made from the ingot of the same composition as seen in figure 6, where the magnetization is plotted as a function of the applied field for various temperatures. The ferromagnetic component is rather large partly because of the unavoidable Ni precipitates always present in Ni-containing alloys [23] and partly because of unknown ferromagnetic impurities since the signal of the sample is small compared to that of the sample holder. This ferromagnetic component ($M = 0.04$ emu g^{-1}) is almost two orders of magnitude higher than that for the ingot ($M = 0.0006$ emu g^{-1}, see figure 5 and table 1). This finding contradicts the expectations that the ribbon produced by a much higher quenching rate should contain less Ni precipitate than the ingot. We explain this discrepancy by the much lower signal-to-noise ratio for the ribbon because of the much smaller sample mass compared to the ingot, giving a large error when correcting for the Langevin diamagnetic component and for the sample holder. By fitting to the high-field part of the curves (solid lines), the susceptibility of the sample ($\chi_{\rm exp}$) can be determined. The inset shows the temperature dependence of $\chi_{\rm exp}$ from which the conduction electron susceptibility, $\chi_{\rm cond}$, is calculated after correction for the Langevin diamagnetic contribution ($\chi_{\rm dia}$). These values are extrapolated to $T = 0$ and the result is summarized in table 1. The conduction electron susceptibility, $\chi^0_{\rm cond} = 23.6 \times 10^{-6}$ emu/molOe for the $Pd_{40}Cu_{30}Ni_{10}P_{20}$ ribbon, differs by roughly a factor of two from that for the ingot of the same composition ($\chi^0_{\rm cond} = 9 \times 10^{-6}$ emu/molOe). Taking into account the huge error for these figures (due to the very low absolute value of the susceptibility, even the sample holder contribution, negligible for the Fe-containing samples, is a source of considerable correction), the conduction electron susceptibility can be regarded as nearly equal in the bulk amorphous ingot and in the amorphous melt-spun ribbon.

Since the susceptibility of the Fe-free Pd-based alloys is quite near to the sensitivity limit of the SQUID magnetometer, a melt-spun binary amorphous ribbon of the composition $Pd_{82}P_{18}$ was also measured as a control sample. This alloy does not contain Ni atoms which are inclined to form giant moments [23], therefore it is expected to be the magnetically most homogeneous alloy in this study. The magnetization of the $Pd_{82}P_{18}$ ribbon is plotted in figure 7 as a function of the applied magnetic field. The susceptibility ($\chi_{\rm exp}$) obtained by fitting a straight line to the high-field portion of the curves (solid lines) is shown in the inset as a function of temperature, together with the conduction electron susceptibility ($\chi_{\rm cond}$) after correction for the Langevin diamagnetic susceptibility ($\chi_{\rm dia}$). The resulting conduction electron susceptibility (extrapolated to $T = 0$, see table 1), $\chi^0_{\rm cond} = 22 \times 10^{-6}$ emu/molOe, for the $Pd_{82}P_{18}$ ribbon is very close to that of the $Pd_{40}Cu_{30}Ni_{10}P_{20}$ ribbon ($\chi^0_{\rm cond} = 23.6 \times 10^{-6}$ emu/molOe). This value for $Pd_{82}P_{18}$ coincides well with the susceptibility value for amorphous $Pd_{80}P_{20}$ extrapolated from the data for amorphous $(Pd_{1-x}Cu_x)_{80}P_{20}$ alloys to $x = 0$ [24, 25].

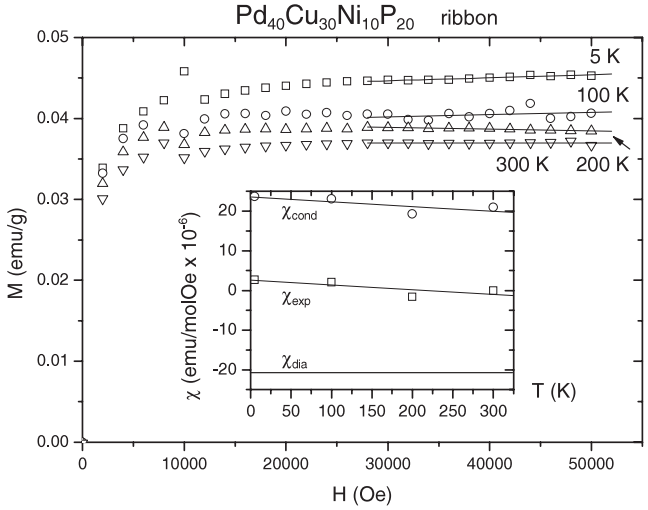

Figure 6. Magnetization as a function of applied field measured at various temperatures for the melt-spun $Pd_{40}Cu_{30}Ni_{10}P_{20}$ ribbon. The solid lines are linear fits between $H = 30$ and 50 kOe. Inset: measured susceptibility ($\chi_{\rm exp}$) versus temperature determined from the fits, temperature-independent Langevin diamagnetic susceptibility ($\chi_{\rm dia}$) and conduction electron susceptibility ($\chi_{\rm cond} = \chi_{\rm exp} - \chi_{\rm dia}$) versus temperature.

4. Discussion

The cluster size calculated in [14] for the melt-spun $Pd_{40}Ni_{22.5}Fe_{17.5}P_{20}$ alloy, which is much larger than that of the giant moments determined for both the $Pd_{35}Cu_{30}Ni_{10}Fe_5P_{20}$ ingot and ribbon used in this study (table 1), is made [14] responsible for the non-saturating character of the $M(H)$ curves. Also, these clusters are associated in [14] with the cusp observed in the magnetization versus temperature curves for low applied fields. The cusp is, however, completely absent in our melt-spun $Pd_{35}Cu_{30}Ni_{10}Fe_5P_{20}$ ribbon in contrast to the ingot of the same composition (figure 4), while both alloys show non-saturating magnetization for high applied fields (figures 1 and 2). This observation excludes any direct links between the clusters and the low-temperature cusp. The cusp thus cannot be an intrinsic property of the amorphous matrix; it should be connected with the precipitates observed in

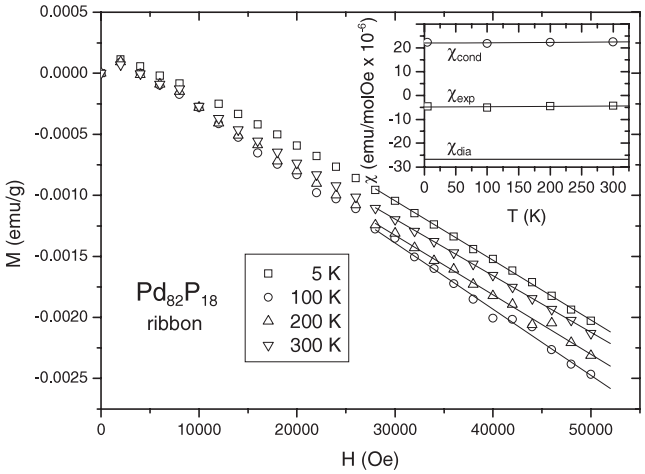

Figure 7. Magnetization as a function of applied field measured at various temperatures for the melt-spun $Pd_{82}P_{18}$ ribbon. The solid lines are linear fits between $H = 30$ and 50 kOe. Inset: measured susceptibility (χ_{exp}) versus temperature determined from the fits, temperature-independent Langevin diamagnetic susceptibility (χ_{dia}) and conduction electron susceptibility ($\chi_{cond} = \chi_{exp} - \chi_{dia}$) versus temperature.

our ingot [15, 16]. These precipitates should be distinct from the giant moments present both in the ingot and the ribbon, the latter being responsible for the non-saturating character of the magnetization as a function of the applied field.

The customary Arrott-plot analysis [26] for the determination of the Curie temperature (T_C) is known [27] to lead to overestimated T_C values in spatially heterogeneous ferromagnets or in the presence of strongly magnetic precipitates in a non-magnetic matrix. Therefore, the $T_C = 60$ K value deduced from the Arrott-plot by Shen *et al* [8] for the Curie point of the bulk $Pd_{35}Cu_{30}Ni_{10}Fe_5P_{20}$ ingot can be misleading. Most probably, the alloy contains nanoscale ferromagnetic precipitates inside a homogeneous paramagnetic matrix. The precipitates could not be detected by routine x-ray diffraction and their observation represents a challenge even for high-resolution transmission electron microscopy due to the low atomic number contrast between particle and matrix.

5. Conclusions

The magnetic properties of Pd-based alloys with and without iron in the form of bulk amorphous ingots and melt quenched ribbons of the same composition were investigated. The Fe-doped alloys, both the ingot and the ribbon, contain magnetic inhomogeneities (giant moments) inside the paramagnetic amorphous matrix, causing the non-saturating behavior of the magnetization curves. In addition, nanocrystalline precipitates are distributed inside the amorphous matrix of the ingot (in contrast to the ribbon), leading to a cusp at low temperatures in the temperature dependence of the low-field magnetization. The iron-free Pd-based alloys remain paramagnetic down to the lowest available temperature with a plausible value for the conduction electron susceptibility when compared to binary Pd–P amorphous alloys. It is pointed out that the complex magnetic behavior of Fe-doped Pd-based bulk metallic glasses can be misinterpreted if the presence of nanocrystalline precipitates observed beyond doubt in the 5 at.% Fe content alloy is not taken into account. In our case an explanation of the cusp observed at low temperatures is not possible in terms of a magnetic phase diagram including paramagnetic, superparamagnetic, spin-glass and field-induced ferromagnetic phases since the cusp disappears when the same BMG ingot is quenched into a ribbon with a high cooling rate. Therefore, the interpretation of a complex magnetic phase diagram in terms of intrinsic, atomic-scale interactions in a homogeneous material can only be justified if the presence of nanometer-scale inhomogeneities in the alloy can be definitively ruled out.

Acknowledgments

The work has been carried out in the framework of the Hungarian–Greek S&T Cooperation (project no. TÉT-GR/06). The $Pd_{82}P_{18}$ amorphous ribbon was prepared during a research stay by one of the authors (IB) at the MPI für Metallforschung, Stuttgart, where he benefited from the kind cooperation of M Ellner (ingot preparation) and F Sommer (preliminary DSC analysis).

References

[1] Drehmann A J and Greer L 1984 *Acta Metal.* **32** 323
[2] Inoue A, Nishiyama N and Matsuda T 1996 *Mater. Trans. JIM* **37** 181
[3] Nishiyama N and Inoue A 1996 *Mater. Trans. JIM* **37** 1531
[4] Mattern N, Sakowski J, Kühn U, Vinzelberg H and Eckert J 2004 *J. Non-Cryst. Solids* **345/346** 758
[5] He Y, Schwarz R B and Archuleta J I 1996 *Appl. Phys. Lett.* **69** 1861
[6] Shen T D, He Y and Schwarz R B 1999 *J. Mater. Res.* **14** 2107
[7] Alamgir F M, Jain H, Williams D B and Schwarz R B 2003 *Micron* **34** 433
[8] Shen T D, Schwarz R B and Thompson J D 1999 *J. Appl. Phys.* **85** 4110
[9] Shen T D, Schwarz R B, Coulter J Y and Thompson J D 2002 *J. Appl. Phys.* **91** 5240
[10] Miller M K, Shen T D and Schwarz R B 2003 *J. Non-Cryst. Solids* **317** 10
[11] Kilcoyne S H, Bentley P M and Greig D 2004 *J. Magn. Magn. Mater.* **272–276** 1383
[12] Kilcoyne S H, Greig D and Gona M N 2005 *Hyperfine Interact.* **165** 167
[13] Yu D H, Fitzsimmons M R, Gilbert E P, Woodward R C, Kilcoyne S H and Robinson R A 2007 *Physica* B **397** 30
[14] Hsiao A C, Lewis L H, Kang K and Moodenbaugh A R 2006 *J. Appl. Phys.* **99** 08F117
[15] Kapaklis V, Schweiss P and Politis C 2005 *Adv. Eng. Mater* **7** 123
[16] Kapaklis V, Poulopoulos P, Wilhelm F, Jaouen N, Rogalev A and Politis C 2005 *J. Appl. Phys.* **98** 044319
[17] Lu Z P, Liu C T and Dong Y D 2004 *J. Non-Cryst. Solids* **341** 93
[18] Crangle J and Scott W R 1965 *J. Appl. Phys.* **36** 921
[19] Fujii H, Hokabe T, Fujiwara H and Okamoto T 1978 *J. Phys. Soc. Japan* **44** 96
[20] Benkowitsch J and Winter H 1983 *J. Phys. F: Met. Phys.* **13** 991

[21] Banhart J, Ebert H, Voitländer J and Winter H 1986 *J. Magn. Magn. Mater.* **61** 221
[22] Selwood W 1956 *Magnetochemistry* (New York: Interscience)
[23] Bakonyi I, Burgstaller A, Socher W, Voitländer J, Tóth-Kádár E, Lovas A, Ebert H, Wachtel E, Willmann N and Liebermann H H 1993 *Phys. Rev.* B **47** 14961
[24] Tangonan G 1976 *PhD Thesis* California Institute of Technology
[25] Johnson W L, Poon S J, Durand J and Duwez P 1978 *Phys. Rev.* B **18** 206
[26] Arrott A 1957 *Phys. Rev.* **108** 1394
[27] Acker F and Huguenin R 1979 *J. Magn. Magn. Mater.* **12** 58